Micro-Macro Behaviour of Granular Materials

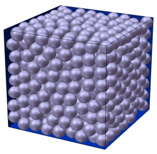

Akke S.J. Suiker
Delft University of Technology
Faculty of Aerospace Engineering
Chair of Engineering Mechanics

Discrete Element Modelling (DEM)

- Research done in collaboration with Norman Fleck, Cambridge University, U.K.
- 3D DEM simulations of particle assemblies to
  - obtain further insight into the *microscopic* and *macroscopic* mechanical behaviour
  - relate material characteristics at micro- and macro levels
- Commercial package 'Particle Flow Code' (Itasca Consulting Group, Minneapolis, U.S.A.)
- Comparison of DEM results with triaxial tests on steel balls (Davy and Fleck)

em engineering mechanics TU Delft

Model Configuration

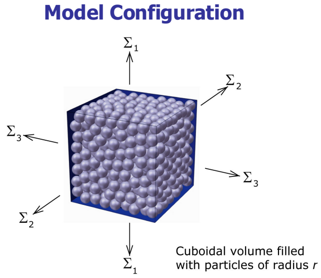

Cuboidal volume of randomly packed, equi-sized, cohesionless spheres (initial porosity is 0.382).

em engineering mechanics TU Delft

Model Characteristics

- Particle interaction by Hertz contact law combined with *Coulomb friction law*:

$$\left| f_d^c \right| = -f_n^c \tan \varphi^c$$

- Dynamic response of particles: explicit time-stepping scheme
- Incremental step is chosen very small to minimise inertia forces (quasi-static analysis) and error accumulation (> 10^5 incremental steps for generating 5% deformation)
- The loading occurs either

strain-controlled or *stress-controlled*

$$\dot{u}_i^{wall} = \dot{E}_{ij} L_j \qquad \dot{u}_i^{wall} = g_j (\Sigma_{ij} - \Sigma_{ij}^{des})$$

Stress and Strain Parameters

Assembly stress is computed as:

$$\Sigma_{ij} = \frac{1}{2V} \sum_{c=1}^{C} f_j^c l_i^c + f_i^c l_j^c$$

Hydrostatic and deviatoric stress invariants:

$$\Sigma^{hydr} = \frac{1}{3} \Sigma_{kk} \qquad \Sigma^{dev} = \sqrt{\frac{3}{2} \Sigma'_{ij} \Sigma'_{ij}} \qquad \text{with} \quad \Sigma'_{ij} = \Sigma_{ij} - \Sigma^{hydr} \delta_{ij}$$

Volumetric and deviatoric strain rate invariants:

$$\dot{E}^{vol} = \dot{E}_{kk} \qquad \dot{E}^{dev} = \sqrt{\frac{2}{3} \dot{E}'_{ij} \dot{E}'_{ij}} \qquad \text{with} \quad \dot{E}'_{ij} = E_{ij} - \frac{1}{3} E^{vol} \delta_{ij}$$

Effect of particle size

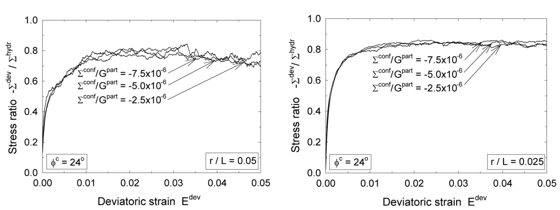

Stress-strain response under axi-symmetric compression
left: r/L =0.05 (1145 particles), right: r/L = 0.025 (9167 particles)

Deformation Characteristics

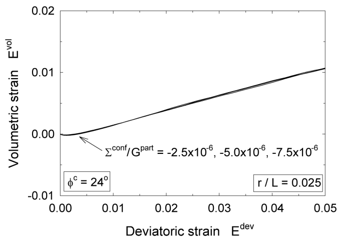

Deviatoric strain versus volumetric strain (r/L=0.025)

Stress-strain Response at various Contact Friction

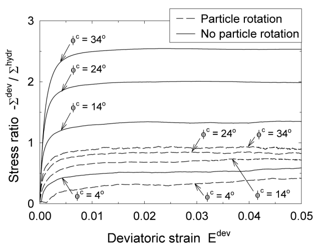

Stress-strain response for various contact friction angles

Deformation Characteristics at various Contact Friction

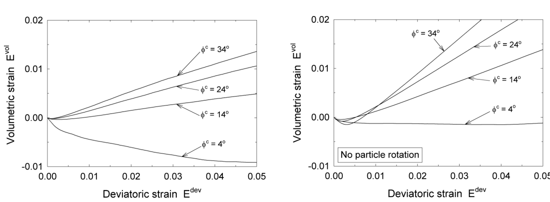

left: particle rotation allowed
right: particle rotation prohibited

Internal Variables at various Contact Friction (at steady-state failure)

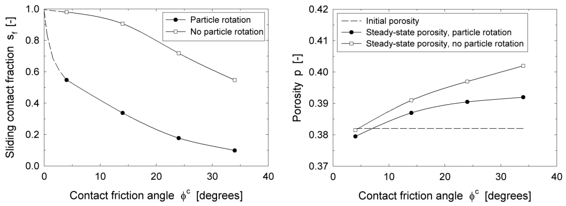

left: Sliding contact fraction versus contact frictions

right: Porosity versus contact friction

engineering mechanics

TU Delft

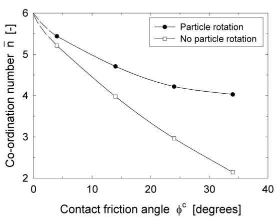

The *minimal* average co-ordination number for obtaining d-dimensional static packings that are stable against external perturbations are

- Frictionless particles $\bar{n}_{\min}$ = 2d (=6)
- Frictional particles $\bar{n}_{\min}$ = d+1 (=4)

(S. Alexander, Phys. Rep. **296**, 1998; S.F. Edwards, Physica A, **249**, 1998)

Co-ordination number versus contact friction angle

engineering mechanics

TU Delft

Effect of Contact Friction on Sample Strength and Dilatancy

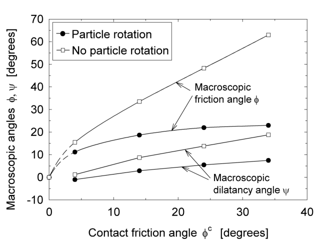

Macroscopic friction and dilatancy angles versus contact friction angle

engineering mechanics

TU Delft

Comparison of DEM Results with Experiments (Davy & Fleck)

- Triaxial loading on cylindrical sample of equi-sized, steel spheres
- Sphere diameter: 4.5 mm
- Sample size: 50 mm diameter, 50 mm height (r/L = 0.045)
- Three states were considered:
  - spheres as received
  - spheres lubricated by PFTE spray
  - braze-coated spheres
- Porosity of test samples was between 0.388 and 0.402

Effect of Contact Friction on Sample Strength

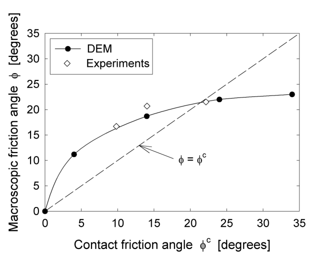

Macroscopic friction angle versus contact friction angle

Effect of Particle Redistribution

Three different kinematic conditions:

- Particle sliding and particle rotation are allowed
- Particle sliding is allowed, particle rotation is prevented
- Particle sliding is allowed in correspondence with an *affine deformation field*, particle rotation is prevented.

Stress-strain Responses

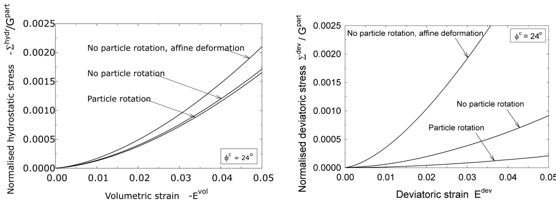

left: Volumetric strain versus hydrostatic stress
(volumetric deformation path $\dot{E}_{11} = \dot{E}_{22} = \dot{E}_{33}$)

right: Deviatoric strain versus deviatoric stress
(deviatoric deformation path $\dot{E}_{11} = -\frac{1}{2}\dot{E}_{22} = -\frac{1}{2}\dot{E}_{33}$)

Continuum failure models

Mohr-Coulomb model

$$F = \Sigma^{hydr}\sin\varphi + \frac{\sqrt{3}}{3}\Sigma^{dev}\sin\left(\theta+\frac{\pi}{3}\right) + \frac{\Sigma^{dev}}{3}\cos\left(\theta+\frac{\pi}{3}\right)\sin\varphi = 0$$

with $\cos 3\theta = \frac{27}{2}\frac{J_3}{\left(\Sigma^{dev}\right)^3}$ where $J_3 = \frac{1}{3}\Sigma'_{ik}\Sigma'_{kj}\Sigma'_{ji}$

Drucker-Prager model

$$F = \Sigma^{dev} + \frac{6\sin\varphi}{3-\sin\varphi}\Sigma^{hydr} = 0$$

Lade-Duncan model

$$F = 27\left(\Sigma^{hydr}\right)^3 - k_1 I_3 = 0$$

with $I_3 = \frac{1}{3}\Sigma_{ij}\Sigma_{jk}\Sigma_{ki} - \frac{1}{2}\Sigma_{kk}\Sigma_{ij}\Sigma_{ji} + \frac{1}{6}\left(\Sigma_{kk}\right)^3$ and $k_1 = \hat{k}_1\left(\frac{\Sigma_2-\Sigma_3}{\Sigma_1-\Sigma_3},\varphi\right)$

Collapse Contour in the Deviatoric Plane

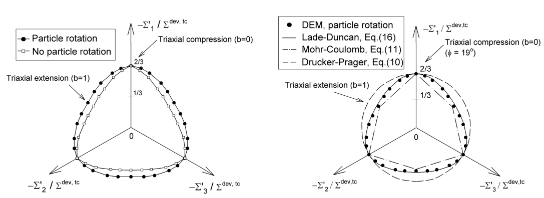

Left: Collapse contour for unconstrained and constrained particle rotation ($\phi^c = 24^0$)

Right: Collapse contour for DEM model (unconstrained particle rotation) and various continuum models

Concluding Remarks

Results presented were taken from:

- A.S.J. Suiker & N.A. Fleck, (2004), Frictional Collapse of Granular Assemblies, *J. Appl. Mech.* **71**, pp. 350-358.

The provision of triaxial test data by Dr. Catherine Davy is gratefully acknowledged

A.S.J.S. and N.A.F. gratefully acknowledge *EU financial support* in the form of *TMR* and *RTN grants* ERB-4061-PL-95-0988 and HPRN-CT-2002-00198 (DEFINO)